

An extended analysis for a generalized Chaplygin gas model

Abdulla Al Mamon*

*Department of Physics, Vivekananda Satavarshiki
Mahavidyalaya (affiliated to the Vidyasagar University),
Manikpara-721513, West Bengal, India*

Andronikos Paliathanasis[†]

*Institute of Systems Science, Durban University of Technology,
PO Box 1334, Durban 4000, Republic of South Africa and
Instituto de Ciencias Físicas y Matemáticas,
Universidad Austral de Chile, Valdivia 5090000, Chile*

Subhajit Saha[‡]

Department of Mathematics, Panihati Mahavidyalaya, Kolkata 700118, West Bengal, India

In this work, we have extended the analysis on the generalized Chaplygin gas (GCG) model as the unification of dark energy and dark matter. Specifically, we have shown that the model of our consideration known as the new generalized Chaplygin gas (NGCG) model, admits a scalar field description, which means that there exist a minimally coupled scalar field for a given scalar field potential where the equation of state is that of the NGCG. With the use of the later property we can construct the slow-roll parameters and derive the corresponding values for the spectral indices for the tensor to scalar perturbation and for the density perturbations. We have also analyzed the behavior of the NGCG model at the perturbation level. In particular, we have studied the growth rate of matter perturbations in terms of evolution of the linear matter density contrast. Using the growth rate data, we then compared our results with the predictions of the concordance Λ CDM and GCG models. Finally, with a view to put the NGCG model on a firm theoretical ground, we have studied the implications of gravitational thermodynamics with the dynamical apparent horizon as the causal boundary. In particular, we have studied the viability of the generalized second law of thermodynamics by assuming that the dynamical apparent horizon in a NGCG universe is endowed with Hawking temperature and Bekenstein entropy.

Keywords: Cosmology; Generalized Chaplygin gas; Inflation; Growth rate; Generalized second law

I. INTRODUCTION

The currently observed accelerated expansion phase of the Universe is widely supported by different observational data [1–5]. In the Einstein theory of gravity, dark energy (DE), a hypothetical exotic fluid, might be responsible for this cosmic acceleration and we refer the interested reader to [6–8] for a detailed description of DE. Observations have long shown that only a small fraction of the total energy density in the Universe is in the form of baryonic matter (around 5%) , with the dark matter (DM) needed for structure formation accounting for about another 26% and the dominant component, DE, brings the total close to the critical density [9]. The simplest model for DE is the standard Λ CDM. The inclusion of cosmological constant Λ with CDM (Cold-Dark-Matter) brings the Λ CDM model into excellent agreement with the observed data. A cosmological constant is described by a single parameter, whose energy density remains constant with time and its equation of state (EoS) parameter is $\omega_\Lambda = -1$. Despite the great success of Λ CDM model, the cosmological constant suffers from the *fine tuning* problem [10] and the *cosmic coincidence* problem [11]. For a recent discussion of the Λ CDM model we refer the reader to [12]. To overcome these issues, various DE models were explored in the literature, which include quintessence, K-essence, phantom, tachyon and so on (for review see [6] and the references therein). However, we do not yet have a satisfactory DE model.

As is well known, the Chaplygin gas (CG) model as a unification of the unknown dark sectors (DM and DE) in Universe is a good candidate among different DE models [13, 14]. In the CG model, the dark sectors can be unified by using an exotic equation of state (EoS) parameter. The striking property of this unified model is that the CG behaves as a dust-like matter (pressureless DM) at early times and behaves like a cosmological constant at late times. But, the CG models are under strong observational pressure from CMB anisotropies

*Electronic address: abdulla.physics@gmail.com

†Electronic address: anpaliat@phys.uoa.gr

‡Electronic address: subhajit1729@gmail.com

[15, 16]. To alleviate this situation, Bento et al. [17, 18] introduced the generalized chaplygin gas (GCG) model with the equation of state $p = -\frac{A}{\rho^\alpha}$ where $A > 0$, α is a real number and it covers original CG for $\alpha = 1$. Like the CG, the GCG also mimics a pressureless matter at early times, while at late times it mimics a cosmological constant. The GCG model has been widely studied in the literature and has confronted with different phenomenological tests involving type Ia supernovae (SNIa), cosmic microwave background (CMB) and other observational datasets [19–24]. Furthermore, it should be noted that the GCG model can be portrayed as an interacting Λ CDM model [24] in which a cosmological constant type DE interacts with cold DM. However, since the EoS parameter of DE still cannot be determined exactly, the observational data show ω_X is in the range of $(-1.2 \leq \omega_X \leq -0.61)$ [25], the GCG model should naturally be generalized to accommodate any possible X-type DE with constant EoS parameter. Later, Zhang et al. [26] proposed the extension version of the GCG, where they called it then as the new generalized Chaplygin gas (NGCG) model, in order to describe the unification of DE and DM, and also demonstrated that the NGCG actually is a kind of interacting XCDM (X-matter with cold DM) model. In this new model, the interaction between the dark sectors is characterized by a constant EoS parameter ω_X . The basic and interesting properties of this new model are discussed in section II. Also, the studies on this new GCG and its applications in cosmology can be found in [26–32]. Recently, Salahedin et al. [31] obtained tight constraints on the the free parameters of NGCG model based on the statistical Markov Chain Monte Carlo method by using various combinations of the latest observational data samples including the SNIa, CMB, Baryon acoustic oscillation (BAO), Big Bang nucleosynthesis (BBN) and the Hubble parameter. Additionally, they also showed that the big tension between the low-redshift and the high-redshift observations appearing in the flat Λ CDM model to predict the current value of Hubble constant can be alleviated in this new model. In an another recent work, Mamon et al. [32] extended the analysis on the NGCG model by performing the statefinder [33, 34] and O_m [35, 36] diagnostic analysis to differentiate the NGCG model from other DE models. Furthermore, they studied the evolutions of the distance modulus and the Hubble parameter for this model and the standard Λ CDM model and compared that with a different combination of observational datasets.

On the other hand, CG and GCG models play an important role for the description

of inflation [54–57]. During the inflationary period it is assumed that the Universe is dominated by a scalar field known as inflaton. In the slow-roll regime of the scalar field dynamics inflation occurs. It was found that various GCG models can be described by the scalar field dynamics with a slow-roll regime. Motivated by these facts, in the present work, we determine the scalar field equivalence for this model while we determine the slow-roll parameters and the spectral indices provided by the NGCG model. We then studied the behavior of this model at the perturbation level as well. More specifically, we study the growth rate of matter perturbations in terms of evolution of the linear matter density contrast and explain how the growth rate data can be used to obtain predictions on the theoretical model under consideration. We also compare our results with the predictions of the standard Λ CDM and GCG models. Furthermore, we also study the viability of the generalized second law of thermodynamics in the NGCG model by assuming that the dynamical apparent horizon is endowed with Hawking temperature and Bekenstein entropy.

The rest of this paper is organized as follows. In the next section, the NGCG model as the unification of DE and DM is introduced briefly. In section III, we investigate the NGCG as candidate for the description of inflation. In section IV, we study the influence of this model on the structure formation. Moreover, in section V, we study the generalized second law of thermodynamics in the NGCG model at the dynamical apparent horizon with a view to garner support for the thermodynamic viability of the NGCG model. Finally, some conclusions are provided in section VI.

Throughout the paper, we use natural units such that $c = G = \hbar = 1$.

II. NEW GENERALIZED CHAPLYGIN GAS (NGCG) MODEL

In this section, we briefly introduce the NGCG model. For details of this model, see for instance Ref. [26]. Assuming the Universe is flat with the Friedmann-Lemaître-Robertson-Walker (FLRW) metric, the EoS of NGCG fluid is given by [26]

$$p_{NGCG} = -\frac{\tilde{A}(a)}{\rho_{NGCG}^\alpha}, \quad (1)$$

where, α is the constant parameter and $\tilde{A}(a)$ is a function depends upon the scale factor (a) of the Universe. It might be expected that the NGCG fluid smoothly interpolates between a dust dominated phase ($\rho \sim a^{-3}$, when a is small) and a DE dominated phase ($\rho \sim a^{-3(1+\omega_{de})}$, when a is large), where ω_{de} is a constant EOS parameter. Also, the energy density of the NGCG fluid can be elegantly expressed as [26]

$$\rho_{NGCG} = [Aa^{-3(1+\omega_{de})(1+\alpha)} + Ba^{-3(1+\alpha)}]^{1/(1+\alpha)} \quad (2)$$

where, A and B are positive constants. Notice that the derivation of the Eq. (2) should be the consequence of substituting the EoS Eq. (1) into the energy conservation equation of the NGCG fluid, this requires the function $\tilde{A}(a)$ to be of the form

$$\tilde{A}(a) = -\omega_{de}Aa^{-3(1+\omega_{de})(1+\alpha)} \quad (3)$$

Finally, from Eq. (2) it follows

$$\rho_{NGCG} = \rho_{NGCG0}a^{-3}[1 - A_s + A_s a^{-3\omega_{de}(1+\alpha)}]^{1/(1+\alpha)} \quad (4)$$

where, $A_s = \frac{A}{A+B}$ and $\rho_{NGCG0} = (A+B)^{1/(1+\alpha)}$ denotes the present value of ρ_{NGCG} . For the NGCG model, as a scenario of the unification of DE and DM, the NGCG fluid is decomposed into two components: the DE component and the DM component, i.e., $\rho_{NGCG} = \rho_{de} + \rho_{dm}$ and $p_{NGCG} = p_{de}$. Therefore, the energy density of the DE and the DM ingredients can be respectively obtained as [26]

$$\rho_{de} = \rho_{de0}a^{-3[1+\omega_{de}(1+\alpha)]} \times [1 - A_s + A_s a^{-3\omega_{de}(1+\alpha)}]^{1/(1+\alpha)-1} \quad (5)$$

$$\rho_{dm} = \rho_{dm0}a^{-3} \times [1 - A_s + A_s a^{-3\omega_{de}(1+\alpha)}]^{1/(1+\alpha)-1} \quad (6)$$

where, ρ_{de0} and ρ_{dm0} represent the present values of ρ_{de} and ρ_{dm} , respectively. It is remarkable that the NGCG model reduces to the standard Λ CDM model when we put $\alpha = 0$ and $\omega_{de} = -1$. We can easily see that it becomes GCG model when $\omega_{de} = -1$. On the other hand, the ω CDM model corresponds to the case $\alpha = 0$. From Eqs. (5) and (6), one can now easily obtains the scaling behavior of the energy densities as

$$\frac{\rho_{dm}}{\rho_{de}} = \frac{\rho_{dm0}}{\rho_{de0}} a^{3\omega_{de}(1+\alpha)} \quad (7)$$

It is evident from the above expression that for $\alpha \neq 0$, there must exist an energy flow between the DE and DM sectors. For example, the energy is transferred from DE to

DM when $\alpha < 0$. On the contrary, the energy is transferred from DM to DE, if $\alpha > 0$. Therefore, α describes the interaction between DM and DE in this model.

Here, we assume a homogeneous, isotropic and spatially flat FLRW Universe filled by NGCG fluid (dark energy plus dark matter), baryonic matter and radiation, then the Friedmann equation can be expressed as

$$3H^2 = \rho_{NGCG} + \rho_b + \rho_r \quad (8)$$

where ρ_b and ρ_r indicates the baryonic matter energy density and the radiation energy density, respectively. The dimensionless Friedmann equation $E(a)$ can be written as

$$E(a) = \frac{H(a)}{H_0} = [(1 - \Omega_{b0} - \Omega_{r0})a^{-3} \times [1 - A_s(1 - a^{-3\omega_{de}\eta})]^{\frac{1}{\eta}} + \Omega_{b0}a^{-3} + \Omega_{r0}a^{-4}]^{\frac{1}{2}} \quad (9)$$

where, $\eta = (1+\alpha)$ and H_0 is the value of the Hubble parameter $H(z)$ at the present epoch. In the above equation, Ω_{b0} and Ω_{r0} denotes the present values of dimensionless energy densities of baryonic matter and radiation, respectively.

III. NGCG AS INFLATIONARY MODEL

In this section, we investigate the NGCG (1) as candidate for the description of the early acceleration phase of the Universe known as inflation. Fluids with equation of state parameters which are generalizations of the CG have been widely applied in the literature as inflationary models see for instance [54–57] and references therein.

In order to perform such analysis we study if the NGCG model can be described by a quintessence scalar field such that the slow-roll description for the inflation to exist. Then, we define the slow-roll parameters and we calculate the values for the spectral indices and we compare with the observations as they are provided by Planck collaboration.

A. Scalar field description

Assume now a spatially flat FLRW spacetime where the matter source is described by a homogeneous scalar field minimally coupled to gravity [58], the inflaton field, such that the

Einstein's field equations to be derived

$$3H^2 = \frac{1}{2}\dot{\phi}^2 + V(\phi), \quad (10)$$

$$2\dot{H} + 3H^2 = -\frac{1}{2}\dot{\phi}^2 + V(\phi), \quad (11)$$

where $\rho_\phi = \frac{1}{2}\dot{\phi}^2 + V(\phi)$, $p_\phi = \frac{1}{2}\dot{\phi}^2 - V(\phi)$ and the continuous equation $\dot{\rho}_\phi + 3H(\rho_\phi + p_\phi) = 0$ reads

$$\ddot{\phi} + 3H\dot{\phi} + V_{,\phi} = 0. \quad (12)$$

Function $V(\phi)$ is the scalar field potential and defines the evolution of the scalar field and the description of the inflationary period, for some examples we refer the reader in [59–61].

We follow the analysis presented in [56] where we are able to write the algebraic solution for the field equations (10)-(12). Indeed, in the new change of variables $dt = \exp\left(\frac{F(x)}{2}\right) d\chi$ with $\chi = 6 \ln a$, the background space reads

$$ds^2 = -e^{F(x)} d\chi^2 + e^{x/3}(dx^2 + dy^2 + dz^2). \quad (13)$$

where the scalar field $\phi(\chi)$ and the scalar field potential $V(\phi(\chi))$ are given by the formulas

$$\phi(\chi) = \pm \frac{\sqrt{6}}{6} \int \sqrt{F'(\chi)} d\chi, \quad (14)$$

$$V(\chi) = \frac{1}{12} e^{-F(\chi)} (1 - F'(\chi)), \quad (15)$$

in which a prime “'” denotes total derivative with respect to χ , i.e. $F'(\chi) = \frac{d}{d\chi} F(\chi)$. The corresponding Hubble function is defined as $H(\chi) = \frac{1}{6} \sqrt{e^{-F(\chi)}}$.

In the new variables the energy density and pressure component are expressed $\rho_\phi(\chi) = \frac{1}{12} e^{-F(\chi)}$, $p_\phi(\chi) = \frac{1}{12} e^{-F(\chi)} (2F'(\chi) - 1)$. Furthermore, the EoS parameter is defined $w_{eff}(\chi) = (2F'(\chi) - 1)$.

Hence, from the EoS parameter (1) we define the ordinary differential equation

$$\frac{1}{12} e^{-F(\chi)} (2F'(\chi) - 1) = \omega_{de} A e^{\chi - \frac{2}{2}(1+\omega_{de})(1+\alpha)} \left(\frac{1}{12} e^{-F(\chi)} \right)^\alpha \quad (16)$$

with analytic solution

$$F(\chi) = \frac{1 + \omega_{de}}{2} \chi - \frac{1}{1 + \alpha} \ln \left(\bar{A} + \exp \left(\frac{(1 + \alpha) \omega_{de}}{2} \chi \right) \right), \quad \alpha \neq -1. \quad (17)$$

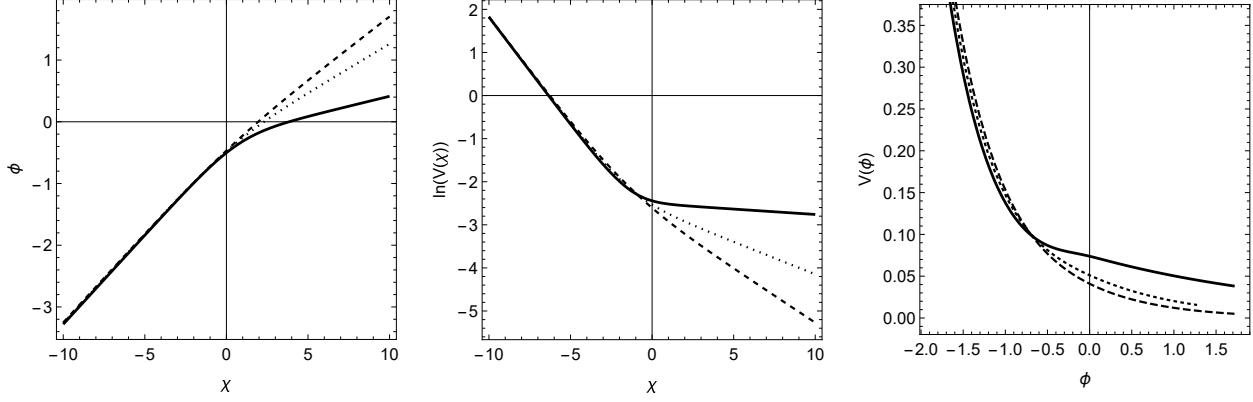


FIG. 1: Qualitative evolution for the scalar field $\phi(\chi)$ (left Fig.) and the scalar field potential $V(\chi)$ (middle Fig.). Plots are for $\bar{A} = 1$ and $\alpha = 1$. Solid lines are for $\omega_{de} = -0.95$, dotted lines are for $\omega_{de} = -0.7$ and dashed lines are for $\omega_{de} = -0.5$. Right figure is the parametric plot $\phi(\chi) - V(\phi(\chi))$.

where $\bar{A} = 12^{-(1+\alpha)}A$. Consequently, for the scalar field we calculate

$$\phi(\chi) = \frac{1}{2\sqrt{3}(1+\alpha)\omega_{de}} \left((1+\alpha)\omega_{de}\sqrt{1+\omega_{de}}\chi - 2\sqrt{1+\omega_{de}} \ln(2\bar{A}(1+\omega_{de}) + \phi_1(\chi)) + 2\ln(\phi_2(\chi)) \right), \quad (18)$$

$$V(\chi) = \frac{1}{24} e^{-\frac{1+\omega_{de}}{2}\chi} \left(\bar{A} + e^{\frac{1+\omega_{de}}{2}\chi} \right)^{-1+\frac{1}{1+\alpha}} \left(\bar{A}(1-\omega_{de}) + e^{\frac{1+\omega_{de}}{2}\chi} \right), \quad (19)$$

with

$$\phi_1(\chi) = (2+\omega_{de}) e^{\frac{1+\omega_{de}}{2}\chi} + 2\sqrt{(1+\omega_{de}) \left(\bar{A} + e^{\frac{1+\omega_{de}}{2}\chi} \right) \left(\bar{A}(1+\omega_{de}) + e^{\frac{1+\omega_{de}}{2}\chi} \right)}, \quad (20)$$

$$\phi_2(\chi) = (2+\omega_{de})\bar{A} + 2 \left(e^{\frac{1+\omega_{de}}{2}\chi} + \sqrt{\left(\bar{A} + e^{\frac{1+\omega_{de}}{2}\chi} \right) \left(\bar{A}(1+\omega_{de}) + e^{\frac{1+\omega_{de}}{2}\chi} \right)} \right). \quad (21)$$

In Fig. 1 we present the qualitative evolution for the scalar field which is equivalent for the NGCG of our consideration. We remark that there exists a real scalar field and a positive valued scalar field potential which provides the same evolution for the background space as the NGCG model. Furthermore, in Fig. 2 we present the qualitative evolution for the equation of state parameter $w_{eff}(a)$.

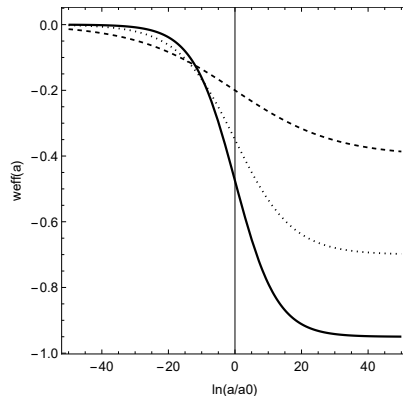


FIG. 2: Qualitative evolution for the equation of state evolution $w_{eff}(a)$ for the NGCG of our consideration. Plot is for $\bar{A} = 1$ and $\alpha = 1$. Solid line is for $\omega_{de} = -0.95$, dotted line is for $\omega_{de} = -0.7$ and dashed line is for $\omega_{de} = -0.5$.

B. Slow-roll parameters and spectral indices

In the inflationary era, the scalar field potential dominates such that $3H^2 \simeq V(\phi)$, while $\dot{\phi} \simeq -\frac{V_{,\phi}}{3H}$. For a specific scalar field potential, the following parameters are defined [62]

$$\varepsilon_V = \left(\frac{V_{,\phi}}{2V}\right)^2, \quad \eta_V = \frac{V_{,\phi\phi}}{2V}, \quad (22)$$

which are known as potential slow-roll parameters. The condition for inflation is $\varepsilon_V \ll 1$, while the additional condition is introduced $\eta_V \ll 1$, such that the inflationary phase to last long enough.

In a similar way, for a specific Hubble function the Hubble slow-roll parameters are defined as follows [62] $\varepsilon_H = -\frac{d \ln H}{d \ln a}$ and $\eta_H = -\frac{d \ln H_{,\phi}}{d \ln a}$. The two different sets of parameters are related as follows $\varepsilon_V \simeq \varepsilon_H$ and $\eta_V \simeq \varepsilon_H + \eta_H$. Consequently, as in the case of the potential slow-roll parameters, the inflationary era is recovered when $\varepsilon_H \ll 1$, while $\eta_H \ll 1$ is the second condition. Because we do not have a closed-form expression for the scalar field potential we select to work with the Hubble slow-roll parameters.

The slow-roll parameters are related with the spectral indices for the density perturbations n_s , and the tensor to scalar ratio r as follows

$$r = 16\varepsilon_H, \quad (23)$$

$$n_s = 1 - 4\varepsilon_H + 2\eta_H. \quad (24)$$

From the analysis of the cosmological observations of the Planck 2018 collaboration [63], the spectral index for the density perturbations is constraint as $n_s = 0.9649 \pm 0.0042$, while the tensor to scalar ratio, r is constraint as $r < 0.10$.

Moreover, we can define the number of e-folds $N_e(\chi)$, by the expression $N_e = \int_{t_i}^{t_f} H(t) dt = \ln \frac{a_f}{a_i} = \frac{1}{6}(\chi_f - \chi_i)$, where χ_f is the moment where the inflation ends, that is, $\varepsilon_H(\chi_f) = 1$.

Thus, the slow-roll parameters r and n_s in the first-order approximation are expressed in term of the number of e-folds as follow

$$r(N_e) = 15 \left(1 - \frac{\omega_{de}}{e^{3(1+\alpha)N_e\omega_{de}} - (1 + \omega_{de})} \right) \quad (25)$$

$$n_s(N_e) = -2 + \frac{3(2 + \alpha)\omega_{de}}{e^{3(1+\alpha)N_e\omega_{de}} - 1} - \frac{3(1 + \alpha)\omega_{de}(1 + \omega_{de})}{(1 + 3\omega_{de})e^{3(1+\alpha)N_e\omega_{de}} - (1 + \omega_{de})}. \quad (26)$$

We observe that $r(N_e)$ and $n_s(N_e)$ are sigmoid functions, where $(1 + \alpha)\omega_{de} < 0$ and for large values of, such as $N_e \simeq 55$ [63], it follows $r \simeq 15(1 + \omega_{de})$ and $n_s \simeq -2 - 3\omega_{de}$. Hence, $\omega_{de} < -0.9933$, where then $n_s \simeq 1$. Hence, the NGCG fits the observations when ω_{de} is near to the cosmological constant term. It is important to mention that we have assumed that α is not close to -1 . Because of the nature of the sigmoid function the behaviour is different when $1 + \alpha \simeq 0$. However, such case is excluded from definition of the model.

Thus, for large values of N_e , it follows that $r(n_s) = 5(1 - n_s)$, where for $n_s \rightarrow 1$, we find $r \rightarrow 0$, which is in agreement with the observations.

IV. GROWTH OF MATTER PERTURBATIONS IN THE NGCG MODEL

In this section, we study the linear growth of DM fluctuations for the NGCG model. Considering the Universe at large scales is homogeneous and isotropic, that it can be described by some modified gravity theory or General Relativity, whose effects at the perturbations level can be taken into account by the effective Newtonian constant [37–49]. Therefore, the matter density perturbations in Fourier space $\delta(a, k)$ depend on the underlying cosmological

model. Using the subhorizon approximation ($k \gg aH$), then it can be shown that the linear matter perturbations grow according to the following second order differential equation [37–46]

$$\delta''(a) + \left(\frac{3}{a} + \frac{H'(a)}{H(a)} \right) - \frac{3}{2} \frac{\Omega_m(a) G_{eff}(a, k)/G_N}{a^2} \delta(a) = 0. \quad (27)$$

where, primes denote differentiation with respect to the scale factor and G_{eff} is the effective Newton constant which is constant and equal to G_N in General Relativity. On the other hand, in general modified gravity models G_{eff} can be dependent on the scale factor (a) and the wave number (k) of the modes of the perturbations in Fourier space. It is important to note that on subhorizon scales ($k \gg aH$), we may ignore the dependence on the wave number k for both G_{eff} and δ [50]. In Eq. (27), $\delta = \frac{\delta\rho_m}{\rho_m}$ denotes the growth function of the linear matter density contrast in which ρ_m represents the background matter density and $\delta\rho_m$ represents its first order perturbation. It deserves to mention here that for the present case, $G_{eff} = G_N$ and $\Omega_m(a) = \Omega_b(a) + \Omega_{dm}(a)$. The corresponding expressions of $\Omega_b(a)$ and $\Omega_{dm}(a)$ are given by

$$\Omega_b(a) = E^{-2}(a) \times \Omega_{b0} a^{-3}, \quad (28)$$

$$\Omega_{dm}(a) = E^{-2}(a) \times \Omega_{dm0} a^{-3} [1 - A_s + A_s a^{-3\omega_{de}\eta}]^{\frac{1}{\eta}-1}, \quad (29)$$

Since we will discuss on low redshifts we ignore the radiation component, i.e. $\Omega_{r0} = 0$. In this case, Eq. (9) becomes

$$E(a) = \frac{H(a)}{H_0} = [(1 - \Omega_{b0})a^{-3} \times [1 - A_s(1 - a^{-3\omega_{de}\eta})]^{\frac{1}{\eta}} + \Omega_{b0}a^{-3}]^{\frac{1}{2}} \quad (30)$$

Next, in order to study the influence of the NGCG model on the structure formation, now we discuss the growth rate f and the root mean square (RMS) normalization of the matter power spectrum σ_8 of the NGCG model. The growth rate can be measured by the peculiar velocities of galaxies falling towards overdense region and is defined as [51–53]

$$f(a) = \frac{d \log \delta}{d \log a}, \quad (31)$$

Also, the RMS fluctuations of the linear density field within spheres of radius $R = 8h^{-1} Mpc$ is defined as

$$\sigma_8(a) = \sigma_{8,0} \frac{\delta(a)}{\delta(1)}, \quad (32)$$

where, $\sigma_{8,0}$ is the present value of $\sigma_8(a)$. However, a more robust and bias free quantity that is measured by redshift surveys is the combination of $f(a)$ and $\sigma_8(a)$. Thus, we have

$$f\sigma_8(a) = a \frac{\delta'(a)}{\delta(1)} \sigma_{8,0}. \quad (33)$$

This observable combination is measured at different redshifts by various cosmological surveys as a probe of the growth of matter density perturbations. Also, the theoretically predicted value of this combination can be evaluated from the solution $\delta(a)$ of the Eq. (27) for a given set of cosmological parameters. Furthermore, one can now compare this theoretical prediction with the observed $f\sigma_8$ dataset. It is evident from Eqs. (27), (28) and (29) that $\delta(a)$ depends on the functional form of $H(a)$ and will give different result when a different $H(a)$ is chosen. Hence, one can easily solve Eq. (27) to determine the evolution of $\delta(a)$ for a given parametrization of $H(a)$ and initial conditions. For the growing mode, we numerically solve the Eq. (27) so that $\delta(a_i) = a_i$ and $\delta'(a_i) = 1$, where, a_i is the initial scale factor which we have chosen to be 10^{-3} . Moreover, we also use in our analysis the best fit values of the free parameters $(\Omega_{b0}, \Omega_{dm0}, \omega_{de}, A_s, \eta) = (0.046, 0.2508, -1.041, 0.7371, 0.9443)$ obtained by Salahedin et al. [31] using $H(z) + \text{BAO} + \text{CMB} + \text{BBN} + \text{SNIa}$ (Pantheon) data. In this work, we have chosen three values of $\sigma_{8,0}$ given by $\sigma_{8,0} = 0.75$ [64], $\sigma_{8,0} = 0.772$ [65] and $\sigma_{8,0} = 0.811$ [66]. Finally, in Fig. 3, we have shown the evolutions of $\delta(z)$ and $f(z)$ for the NGCG model. The plot of δ versus redshift parameter z is shown in the left panel of Fig. 3, while the corresponding plot of $f(z)$ is shown in the right panel of Fig. 3. For comparison, the evolutions of $\delta(z)$ and $f(z)$ for a flat ΛCDM ($\omega_{de} = -1, \eta = 1$) and GCG ($\omega_{de} = -1$) models are also shown. By comparing the evolutionary trajectories in Fig. 3, it has been found that at early times, the δ and f of these three models are the same, but the deviation among these models grows at late times. Furthermore, in Fig. 4, we compared the observed $f(z)\sigma_8(z)$ with the theoretical value of growth rate function for this model. It is observed from Fig. 4 that the present model reproduces the observed values of $f(z)\sigma_8(z)$ quite effectively. It has been found that the nature of the plot does not crucially depend on the value of $\sigma_{8,0}$.

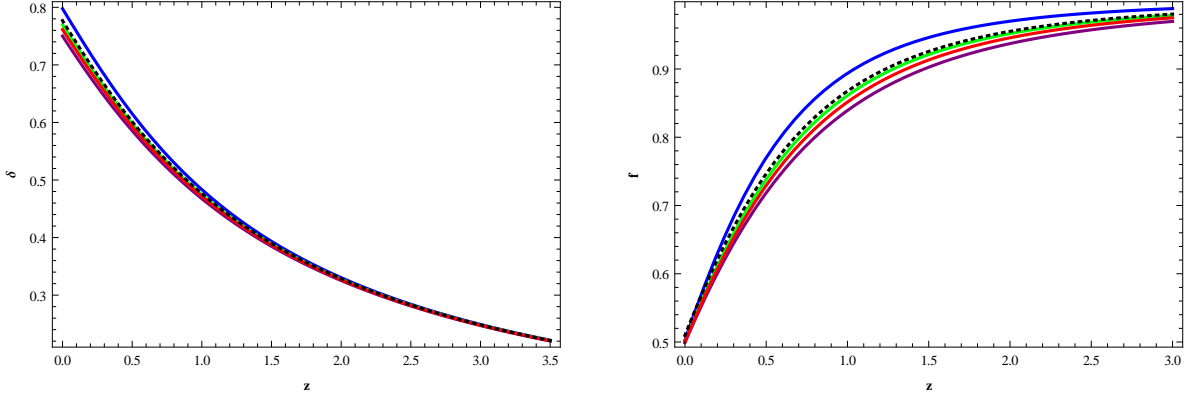


FIG. 3: The evolutionary trajectories of δ (left panel) and f (right panel) are shown as a function of redshift $z(\equiv \frac{1}{a} - 1)$, for the NGCG model by considering the values of $\Omega_{b0} = 0.046, \Omega_{dm0} = 0.2508, A_s = 0.7373$ and $\eta = 0.9443$. The blue, green and purple curves are for $\omega_{de} = -1.2, \omega_{de} = -1.041$ and $\omega_{de} = -0.95$, respectively. In each plot, the black and red curves represent the corresponding evolutions of $\delta(z)$ and $f(z)$ in a Λ CDM ($\omega_{de} = -1, \eta = 1$) and GCG ($\omega_{de} = -1$) models, respectively.

V. GENERALIZED SECOND LAW OF THERMODYNAMICS IN THE NGCG MODEL

In this section, we wish to study the generalized second law in the NGCG model by considering the dynamical apparent horizon as the thermodynamic boundary. It is worthwhile to mention here that the generalized second law was adapted in the context of Cosmology by Brustein [67]. This second law is based on the conjecture that causal boundaries and not only black hole event horizons have geometric entropies proportional to their area. The dynamical apparent horizon always exists irrespective of the cosmological model we choose. This property allows it to be a natural choice for the study of gravitational thermodynamics. The results obtained within this framework can then be extended to the whole Universe, thanks to the cosmological principle.

It must be noted that the dynamical apparent horizon is a thermodynamic entity which must be endowed with an entropy and a temperature. In analogy with a black hole event horizon in the study of black hole thermodynamics [68, 69], the temperature associated with the dynamical apparent horizon is identified as the Hawking temperature whose expression

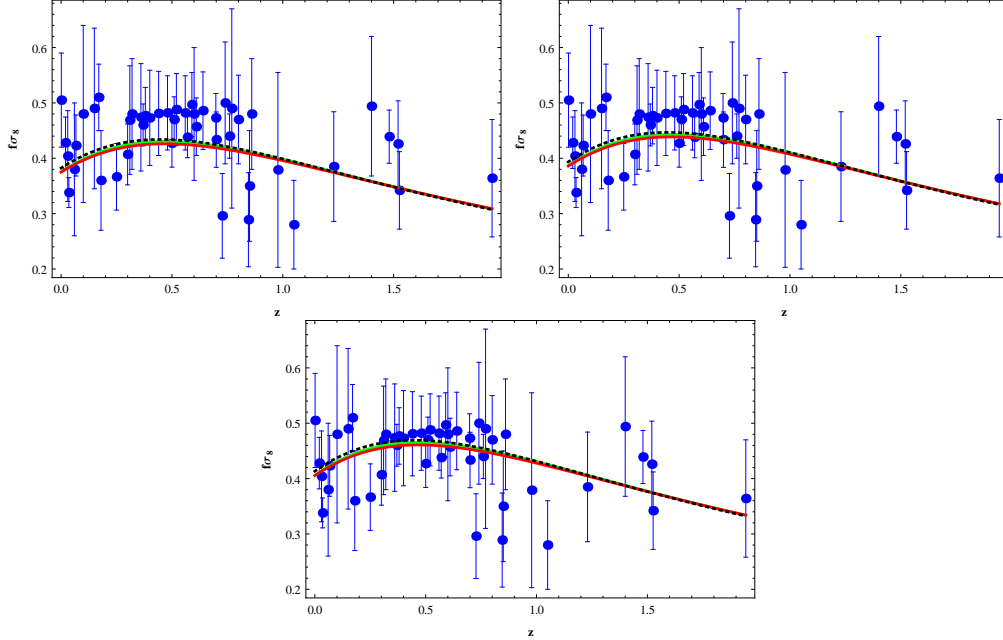


FIG. 4: The evolutionary trajectory of $f\sigma_8$, as a function of redshift z , is shown for the present model (green curve) by considering the values of $\Omega_{b0} = 0.046$, $\Omega_{dm0} = 0.2508$, $\omega_{de} = -1.041$, $A_s = 0.7373$ and $\eta = 0.9443$. The plots are for $\sigma_{8,0} = 0.75$ [64] (left panel), $\sigma_{8,0} = 0.772$ [65] (right panel) and $\sigma_{8,0} = 0.811$ [66] (lower panel), respectively. In each plot, the black and red curves represent the corresponding evolutions of $f\sigma_8$ in a Λ CDM and GCG models, respectively. Also, the blue dots (with the error bars) correspond to the 47 Growth of matter data points (redshift space distortions measurements) in the redshift range $0.001 \leq z \leq 1.944$, obtained from different surveys and the corresponding $f\sigma_8$ values are given in [25] and the relevant references therein.

is given by

$$T_{A_X} = \frac{1}{2\pi R_{A_X}} \left(1 - \frac{\dot{R}_{A_X}}{2} \right), \quad (34)$$

where R_{A_X} is the proper radius of the apparent horizon in the NGCG model. In the rest of this section, the suffix ‘X’ will denote corresponding parameters in a NGCG-dominated universe. One should note that Eq. (34) represents the non-truncated version of the Hawking temperature. It has been customary to use the truncated expression [70]

$$T_{A_X}^{(tr)} = \frac{1}{2\pi R_{A_X}} \quad (35)$$

in the literature for the study of gravitational thermodynamics, however, Binétruy and Helou [71, 72] have put forward several strong arguments against the use of the truncated

Hawking temperature. Furthermore, the consideration of the non-truncated form of the Hawking temperature has presented us with some promising results in a recent paper [73] by one of the authors.

The entropy on the horizon is given by the Bekenstein entropy which has the expression [74]

$$\begin{aligned} S_{A_X} &= \frac{A_{A_X}}{4} \\ &= \pi R_{A_X}^2, \end{aligned} \quad (36)$$

where $A_{A_X} = 4\pi R_{A_X}^2$ is the proper area bounded by the dynamical apparent horizon.

Next, we require the time-derivative of the entropy of the cosmic fluid inside the apparent horizon, which is obtained from the Clausius relation

$$T_{f_{A_X}} dS_{f_{A_X}} = dU + p_{NGCG} dV_{A_X}, \quad (37)$$

where, $S_{f_{A_X}}$ and $T_{f_{A_X}}$ are the entropy and the temperature of the cosmic fluid within the horizon, respectively, while $U = \frac{4}{3}\pi R_{A_X}^3 \rho_{NGCG}$ is the internal energy of the fluid evaluated at the apparent horizon. We shall assume that the temperature of the cosmic fluid, $T_{f_{A_X}}$, is equal to T_{A_X} in Eq. (34). This assumption is supported by the results obtained in the pioneering work by Mimoso and Pavón [75].

Now, using Eqs. (34), (36), and (37), we obtain the time-derivative of the total entropy

$$\dot{S}_{A_X} = 18\pi R_{A_X} \frac{(1 + w_{NGCG})^2}{(1 - 3w_{NGCG})}, \quad (38)$$

which directly follows from Eq. (19) of Ref. [73]. The generalized second law is nothing but the requirement that \dot{S}_{A_X} be non-negative. In our model, this requirement is satisfied if $w_{NGCG} \leq \frac{1}{3}$. It is quite easy to see that the effective EoS of the NGCG model is given by

$$\begin{aligned} w_{NGCG} &= \frac{p_{NGCG}}{\rho_{NGCG}} \\ &= \frac{w_{de}}{1 + \left(\frac{B}{A}\right) a^{3w_{de}(1+\alpha)}}. \end{aligned} \quad (39)$$

Since the constants A and B are both positive, and w_{de} is always negative, it follows that $w_{NGCG} \leq \frac{1}{3}$ is always true. Thus, the generalized second law is unconditionally valid in the NGCG model and consequently, this model is consistent with thermodynamics.

VI. CONCLUSIONS

Cosmological fluids with equation of state similar to that of the Chaplygin Gas have been widely used for the study of the inflation. Moreover, they have been applied for the description of the inflaton field. In this study we show that the model of our consideration, the NGCG model, admits a scalar field description, which means that there exist a minimally coupled scalar field for a given scalar field potential where the equation of state parameter is that of the NGCG. Hence, we were able to determine the slow-roll parameters for the NGCG and determine the spectral indices and compare their values with the observational ones. In the first-order approximation, we derived the closed-form expressions for the scalar to tensor ratio and for the spectral index for the density perturbations. These two indices were found to be functions of the number of e-folds, N_e , and of the two parameters α and ω_{de} of the NGCG model. In addition, the functional form is that of a sigmoid where we found that for $(1 + \alpha)\omega_{de} < 0$ and for large values of the number of e-folds the spectral indices are related by the linear expression $r(n_s) = 5(1 - n_s)$. The later expression provides values for the spectral indices in agreement with the observations.

Furthermore, we studied the growth of matter perturbations in the NGCG scenario. In particular, we have shown the evolutions of the matter density contrast $\delta(z)$ and the growth rate $f(z)$ for this model and compared it with that of the standard Λ CDM and the GCG models. By comparing these models (NGCG, Λ CDM and GCG), we have shown that of these three models are the same at early times, but the evolutionary trajectory of the NGCG model deviates from the other two at late times. We have also computed the combination parameter $f\sigma_8$ (33) as a function of the redshift for this model. The numerical results are summarized in Fig. 4, where the comparison with the redshift space distortions measurements is shown as well.

Finally, we have also shown that the NGCG model is consistent with gravitational thermodynamics, a result which puts the NGCG model on a firm theoretical ground.

-
- [1] A. G. Riess et al., “Observational evidence from supernovae for an accelerating universe and a cosmological constant,” *Astron. J.* **116**, 1009 (1998).
 - [2] S. Perlmutter et al., “Measurements of Ω and Λ from 42 high redshift supernovae,” *Astrophys.*

- J. **517**, 565 (1999).
- [3] P. de Bernardis et al., “A Flat universe from high resolution maps of the cosmic microwave background radiation,” *Nature* **404**, 955 (2000).
- [4] W. J. Percival et al., “The 2dF Galaxy Redshift Survey: The Power spectrum and the matter content of the Universe,” *Mon. Not. Roy. Astron. Soc.* **327**, 1297 (2001).
- [5] D. N. Spergel et al., “First year Wilkinson Microwave Anisotropy Probe (WMAP) observations: Determination of cosmological parameters,” *Astrophys. J. Suppl.* **148**, 175 (2003).
- [6] L. Amendola and S. Tsujikawa, *Dark Energy: Theory and Observations*, Cambridge University Press, Cambridge, UK, (2010).
- [7] K. Bamba, S. Capozziello, S. Nojiri, S. D. Odintsov, “Dark energy cosmology: The equivalent description via different theoretical models and cosmography tests,” *Astrophys. Space Sci.* **342**, 155 (2012).
- [8] E. J. Copeland, M. Sami, S. Tsujikawa, “Dynamics of dark energy,” *Int. J. Mod. Phys. D.* **15**, 1753 (2006).
- [9] P. A. R. Ade et al. [Planck Collaboration], “Planck 2015 results XIV. Dark energy and modified gravity,” *A&A*, **594**, A14 (2016).
- [10] S. Weinberg, “The cosmological constant problem,” *Rev. Mod. Phys.* **61**, 1 (1989).
- [11] P. J. Steinhardt, L. Wang, I. Zlatev, “Cosmological tracking solutions,” *Phys. Rev. D* **59**, 123504 (1999).
- [12] L. Perivolaropoulos and F. Skara, “Challenges for Λ CDM: An update,” [arXiv:2105.05208 [astro-ph.CO]].
- [13] A. Kamenshchik, U. Moschella, V. Pasquier, “An alternative to quintessence,” *Phys. Lett. B* **511**, 265 (2001).
- [14] V. Gorini, A. Kamenshchik, U. Moschella, “Can the Chaplygin gas be a plausible model for dark energy?,” *Phys. Rev. D* **67**, 063509 (2003).
- [15] H.B. Sandvik, M. Tegmark, M. Zaldarriaga, I. Waga, “The end of unified dark matter?,” *Phys. Rev. D* **69**, 123524 (2004).
- [16] R. Bean, O. Dore, “Are Chaplygin gases serious contenders for the dark energy?,” *Phys. Rev. D* **68**, 023515 (2003).
- [17] M.C. Bento, O. Bertolami, A. A. Sen, “Generalized Chaplygin gas, accelerated expansion and dark energy matter unification,” *Phys. Rev. D* **66**, 043507 (2002).

- [18] M.C. Bento, O. Bertolami, A. A. Sen, “Revival of the unified dark energy-dark matter model?,” *Phys. Rev. D.* **70**, 083519 (2004).
- [19] M. C. Bento, O. Bertolami, A. A. Sen, “Generalized Chaplygin gas and CMBR constraints,” *Phys. Rev. D* **67**, 063003 (2003).
- [20] M. C. Bento, O. Bertolami, A. A. Sen, “WMAP Constraints on the Generalized Chaplygin Gas Model,” *Phys. Lett. B* **575**, 172 (2003).
- [21] O. Bertolami, A. A. Sen, S. Sen, P. T. Silva, “Latest Supernova data in the framework of Generalized Chaplygin Gas model,” *Mon. Not. Roy. Astron. Soc.* **353**, 329 (2004).
- [22] J. S. Alcaniz, D. Jain, A. Dev, “High-redshift objects and the generalized Chaplygin gas,” *Phys. Rev. D* **67**, 043514 (2003).
- [23] M. C. Bento, O. Bertolami, N. M. C. Santos, A. A. Sen, “Supernovae constraints on models of dark energy revisited,” *Phys. Rev D* **71**, 063501 (2005).
- [24] T. Barreiro, O. Bertolami, P. Torres, “WMAP five-year data constraints on the unified model of dark energy and dark matter” *Phys. Rev. D* **78**, 043530 (2008).
- [25] D. Benisty, “Quantifying the S_8 tension with the Redshift Space Distortion data set,” *Physics of the Dark Universe* **31**, 100766 (2021).
- [26] X. Zhang, F.Q. Wu, J. Zhang, “New generalized Chaplygin gas as a scheme for unification of dark energy and dark matter,” *JCAP* **0601**, 003 (2006).
- [27] K. Liao, Y. Pan, Z. H. Zhu, “Observational constraints on new generalized Chaplygin gas model” *Res. Astron. Astrophys.* **13**, 159 (2013).
- [28] J. Wang, Y. B. Wu, D. Wang, W. Q. Yang, “The Extended Analysis on New Generalized Chaplygin Gas,” *Chin. Phys. Lett.* **26**, 089801 (2009).
- [29] M. Jamil, “Interacting New Generalized Chaplygin Gas,” *Int. J. Theor. Phys.* **49**, 62 (2010).
- [30] A. Salehi, M. R. Setare, A. Alaii, “Reconstructing cosmographic parameters from different cosmological models: case study. Interacting new generalized Chaplygin gas model,” *Eur. Phys. J. C* (2018) **78**, 495 (2018).
- [31] F. Salahedin, R. Pazhouhesh, M. Malekjani, “Cosmological constrains on new generalized Chaplygin gas model,” *Eur. Phys. J. Plus* **135**, 429 (2020).
- [32] A. A. Mamon, V. C. Dubey, K. Bamba, “Statefinder and O_m Diagnostics for New Generalized Chaplygin Gas Model,” *Universe* **7**, 362 (2021).
- [33] V. Sahni, T. D. Saini, A. A. Starobinsky, U. Alam, “Statefinder—A new geometrical diagnostic

- of dark energy,” J. Exp. Theo. Phy. Lett. **77**, 201 (2003).
- [34] U. Alam, V. Sahni, T.D. Saini, A. A. Starobinsky, “Exploring the Expanding Universe and Dark Energy using the Statefinder Diagnostic,” Mon. Not. R. Astron. Soc. **344**, 1057 (2003).
- [35] V. Sahni, A. Shafieloo, A. A. Starobinsky, “Two new diagnostics of dark energy,” Phys. Rev. D **78**, 103502 (2008).
- [36] C. Zunckel, C. Clarkson, “Consistency Tests for the Cosmological Constant,” Phys. Rev. Lett. **101**, 181301 (2008).
- [37] E. V. Linder, A. Jenkins, “Cosmic Structure Growth and Dark Energy,” Mon. Not. Roy. Astron. Soc. **346**, 573 (2003).
- [38] A. Bueno belloso, J. Garcia-Bellido, and D. Sapone, “A parametrization of the growth index of matter perturbations in various Dark Energy models and observational prospects using a Euclid-like survey,” JCAP **1110**, 010 (2011).
- [39] L. Amendola, M. Kunz and D. Sapone, “Measuring the dark side (with weak lensing),” JCAP, **0804**, 013 (2008).
- [40] S. Nesseris, “Matter density perturbations in modified gravity models with arbitrary coupling between matter and geometry,” Phys. Rev. D **79**, 044015 (2009).
- [41] S. Nesseris, G. Pantazis, L. Perivolaropoulos, “Tension and constraints on modified gravity parametrizations of $G_{eff}(z)$ from growth rate and Planck data,” Phys. Rev. D **96**, 023542 (2017).
- [42] S. Nesseris, D. Sapone, “Accuracy of the growth index in the presence of dark energy perturbations,” Phys. Rev. D **92**, 023013 (2015).
- [43] S. Nesseris, A. Mazumdar, “Newton’s constant in $f(R, R_{\mu\nu}R^{\mu\nu}, \square R)$ theories of gravity and constraints from BBN,” Phys. Rev. D **79**, 104006 (2009).
- [44] S. Tsujikawa, “Matter density perturbations and effective gravitational constant in modified gravity models of dark energy,” Phys. Rev. D **76**, 023514 (2007).
- [45] A. De Felice, S. Tsujikawa, “ $f(R)$ theories,” Living Rev. Rel. **13**, 3 (2010).
- [46] A. De Felice, S. Mukohyama, S. Tsujikawa, “Density perturbations in general modified gravitational theories,” Phys. Rev. D **82**, 023524 (2010).
- [47] H. Steigerwald, J. Bel, C. Marinoni, “Probing non-standard gravity with the growth index: a background independent analysis,” JCAP **05**, 042 (2014).
- [48] G. Papagiannopoulos, S. Basilakos, A. Paliathanasis, S. Savvidou, and P.C. Stavrinos,

- “Finsler-Randers Cosmology: dynamical analysis and growth of matter perturbations,” *Class. Quantum Grav.* **34**, 225008 (2017).
- [49] W. Khyllep, A. Paliathanasis, J. Dutta, “Cosmological solutions and growth index of matter perturbations in $f(Q)$ gravity,” *Phys. Rev. D* **103**, 103521 (2021).
- [50] J. C. Bueno Sanchez, L. Perivolaropoulos, “Evolution of Dark Energy Perturbations in Scalar-Tensor Cosmologies,” *Phys. Rev. D* **81**, 103505 (2010).
- [51] Li-Min Wang, P. J. Steinhardt, “Cluster abundance constraints on quintessence models,” *Astrophys. J.* **508**, 483 (1998).
- [52] E. V. Linder, “Cosmic growth history and expansion history,” *Phys. Rev. D* **72**, 043529 (2005).
- [53] D. Polarski, R. Gannouji, “On the growth of linear perturbations,” *Phys. Lett. B* **660**, 439 (2008).
- [54] J.D. Barrow, “Graduated Inflationary Universe,” *Phys. Lett. B* **235**, 40 (1990).
- [55] J.D. Barrow and P. Saich, “The Behavior of intermediate inflationary universes”, *Phys. Lett. B* **249**, 406 (1990).
- [56] J.D. Barrow and A. Paliathanasis, “Observational Constraints on New Exact Inflationary Scalar-field Solutions,” *Phys. Rev. D* **94**, 083518 (2016).
- [57] J.D. Barrow and A. Paliathanasis, “Reconstructions of the dark-energy equation of state and the inflationary potential,” *Gen. Relativ. Grav.* **50**, 82 (2018).
- [58] P. Ratra and L. Peebles, “Cosmological consequences of a rolling homogeneous scalar field,” *Phys. Rev. D* **37**, 3406 (1988).
- [59] A.R. Liddle, “Chaotic Inflation,” *Phys. Lett. B* **129**, 177 (1983).
- [60] P. Parsons and J.D. Barrow, “Generalised Scalar Field Potentials and Inflation,” *Phys. Rev. D* **51**, 6757 (1995).
- [61] A.R Liddle, A. Mazumdar and F.E. Schunck, “Assisted inflation” *Phys. Rev. D* **58**, 061301 (1998).
- [62] A.R. Liddle, P. Parson and J.D. Barrow, “Formalising the Slow-Roll Approximation in Inflation,” *Phys. Rev. D* **50**, 7222 (1994).
- [63] Y. Akrami et al. [Planck Collaboration], “Planck 2018 results. X. Constraints on inflation,” *A&A* **641**, A10 (2020).
- [64] P. Ade et al. (Planck), “Planck 2013 results. XX. Cosmology from Sunyaev-Zeldovich cluster counts,” *Astron. Astrophys.* **571**, A20 (2014).

- [65] H. Hildebrandt et al., “KiDS-450: Cosmological parameter constraints from tomographic weak gravitational lensing” *Mon. Not. Roy. Astron. Soc.* **465**, 1454 (2017).
- [66] N. Aghanim et al. (Planck), “Planck 2018 results. VI. Cosmological parameters,” *A&A* **641**, A6 (2020).
- [67] R. Brustein, “Generalized second law in cosmology from causal boundary entropy,” *Phys. Rev. Lett.* **84**, 2072 (2000).
- [68] R.M. Wald, “The thermodynamics of black holes,” *Living Reviews in Relativity* **4**, 6 (2001).
- [69] S. Carlip, “Black hole thermodynamics,” *International Journal of Modern Physics D* **23**, 1430023 (2014).
- [70] S.W. Hawking, “Particle creation by black holes,” *Commun. Math. Phys.* **43**, 199 (1975).
- [71] P. Binétruy and A. Helou, “The apparent universe,” *Class. Quantum Grav.* **32**, 205006 (2015).
- [72] A. Helou, “Dynamics of the Cosmological Apparent Horizon: Surface Gravity & Temperature,” arXiv:1502.04235 [gr-qc].
- [73] S. Saha, “Viaggiu entropy and the generalized second law in a flat FLRW universe,” *Int. J. Mod. Phys. A* **34**, 1950193 (2019).
- [74] J.D. Bekenstein, “Black Holes and Entropy,” *Phys. Rev. D* **7**, 2333 (1973).
- [75] J.P. Mimoso and D. Pavón, “Considerations on the thermal equilibrium between matter and the cosmic horizon,” *Phys. Rev. D* **94**, 103507 (2016).